Key Biomarkers Within the Colorectal Cancer Related Inflammatory Microenvironment

Valentin Calu
Carol Davila University of Medicine and Pharmacy
Adriana Ionescu
University of Bucharest
Loredana Stanca
University of Agronomic Sciences and Veterinary Medicine of Bucharest
Ovidiu Geicu
University of Agronomic Sciences and Veterinary Medicine of Bucharest
Florin Iordache
University of Agronomic Sciences and Veterinary Medicine of Bucharest
Aurelia Pisoschi
University of Agronomic Sciences and Veterinary Medicine of Bucharest
Andreea Serban (irensro@yahoo.com)
University of Agronomic Sciences and Veterinary Medicine of Bucharest
Liviu Bilteanu
University of Agronomic Sciences and Veterinary Medicine of Bucharest

Research Article

Keywords: colorectal cancer (CRC), Chitinase, occludin, MMP2

Posted Date: December 9th, 2020

DOI: https://doi.org/10.21203/rs.3.rs-118868/v1

Version of Record: A version of this preprint was published at Scientific Reports on April 12th, 2021. See the published version at https://doi.org/10.1038/s41598-021-86941-5.

Abstract

The necessity of therapeutic approaches focused on the inflammatory microenvironment of colorectal cancer (CRC) is becoming more and more apparent, both in order to improve post-surgical care and subsequent therapeutic strategies, and also for better quality of life for the patients. We have investigated a panel of 39 inflammatory factors using a multiplex magnetic bead-based immunoassay, in relation with CEA and CA19-9, classical tumor markers and the expression levels of pErk, occludin, and STAT1 and STAT3 transcriptional factors. Within the tumor and paired normal tissue samples collected during tumor resection surgery, we have identified 32 biomarkers displaying statistically significant differences. Several relevant correlations have been observed in a combined multi-type correlation matrix. Chitinase 3-like 1 seems to be a trigger for activation pathways for tumor growth and metastasis. Through IL-22 and IL1β, IL-8 correlates indirectly with CA19-9 and CEA, respectively. We also emphasize the diminished APRIL and high BAFF levels in colon cancer tumor tissue, which is quite unique. The strong correlation between APRIL, BAFF, IL-8 and MMP2 recommends these as combined targets in immunotherapies for colon cancer treatment, and indicates the marker quartet may serve as a starting point in colon cancer screening.

Introduction

Colorectal cancer (CRC) is the third most common fatal malignancy worldwide [1], almost 50% of these patients eventually succumbs to the disease. In recent years, there have been major advances in understanding the molecular basis of tumor and its progression from adenoma to carcinoma. These pathways can hold potential for translation into novel strategies for the treatment of CRC [2]. The malignant phenotype activates inflammatory cells leading to cellular immunity alteration and forcing these cells to produce soluble factors (cytokines, chemokines, growth factors, proteases, etc.) that regulate growth, differentiation and survival of tumor cells. Tumor expansion causes thus significant peritumoral inflammation which determines the continuous activation of the pathways involved in tumor initiation, promotion and progression [3]. These stages of neoplastic evolution are enhanced within the inflammatory context which promotes sustained proliferation, resistance to apoptosis, reprogramming and reorganization of the stromal environment, and genomic instability [4]. In addition, tumor cells increase the inflammatory constellation by producing a wide range of cytokines, cytotoxic mediators including reactive oxygen species, serine and cysteine proteases, MMPs and membrane-perforating agents [4,5]. In order to modulate the immune response towards cancer cells and induce, if possible, tumor cell death, cytokines, which are a part of the immune response, are targeted in some types of immunotherapies. However, focusing on a single cytokine was shown to have only moderate efficiency in low doses, while high dose monotherapies lead to significant side effects. The creation of multi-targeted immunotherapies needs a thorough understanding of correlated cytokines actions within the anti-tumor response [6]. Such a need led to investigations of extended panel of inflammatory markers in cancer patients. Molecules such as IL-20, IL-1β and IL-22 have proved important features for being therapeutic targets in CRC [7]. Several studies employing extended multiplexes for inflammatory profiling led to a wide diversity of encouraging

results, for instance IL-6 [8–11] and IL-8 [10–12], expressions are higher in serum patients with CRC, and are currently being considered as candidates to be added as new potential therapeutic targets. Other biomarkers with diagnostic and prognostic value in CRC reported by several studies are IL-8 programmed death ligand 1 (PD-L1)[10] CEA [11,13], CA19-9[12] [7], MMP-9 [13] etc. Despite such a multitude of studies, to date there is no unique panel of biomarkers to distinguish between different types of cancers and more studies are needed to find a reliable panel of biomarkers in terms of sensitivity and specificity for predictive and diagnostic aims. Moreover a combination of these markers could help the understanding the complex chain of molecular phenomena and events leading to this phenotype.

In this work, we describe through statistical correlations some possible molecular pathways involving tumor-related inflammation markers and their association to CRC progression. Molecules that are simultaneously involved in CRC progression through common pathways might be either eligible targets for new immunotherapy drugs aiming to improve life quality and lifespan of CRC patients or grouped in a screening panel guiding CRC patients evolution and the improvement of post-surgical therapies.

Results

Array Data

The level of 39 inflammatory factors in tumor and paired normal tissue collected from CRC patients during tumor resection surgery have been quantified using the Bio-Plex Pro™ assay. In addition, the concentrations of CEA and CA19.19 were detected by ELISA and the protein expression levels of phosphorylated extracellular-regulated kinase ½ (pErk1/2), occludin (OCLN), signal transducer and activator of transcription 1 (STAT1) and 3 (STAT3), and carbonylated proteins (CP) were assessed through immunobloting. The concentrations of the following biomarkers (in alphabetical order) have been under the lowest limit of quantization (LLOQ) or under the limit of detection (LOD): IFN-α2, IL-2, IL-10, IL-11, IL-12p70, IL-19, IL-27(p28), IL-28A/ IFN-λ2, IL-29/IFN-λ1 and osteocalcin.

All the remaining raw data sets which were detected beyond LOD (see Supplementary Table 1), have failed the initial Shapiro-Wilks test. After log-transformation, the levels exhibiting a normal distribution and statistically significant differences in tumor vs. control were (in alphabetical order): APRIL, BAFF, CA19-9, pERK, IL-1β, IL-1RA, IFN-β, IL-26, MMP-2, TSLP and TWEAK (Fig. 1).

All these markers except APRIL, IFN-β and TWEAK, were upregulated in tumor samples compared to controls. The log-transformed levels which were normally distributed but exhibited no difference between tumor tissue and control were those of sCD30.

The log-transformed levels which do not exhibit a normal distribution but exhibit statistically significant differences via Wilcoxon tests were (in alphabetical order): CP, CEA, Chitinase 3-like 1 (CHI3L1), gp130, IFN-γ, IL-8, IL-20, IL-22, IL32, IL-34, IL-35, LIGHT/TNFSF14, OCLN, MMP-1, MMP-3, osteopontin (OPN), sIL-6Rα, STAT1, STAT3, sTNFR1 and sTNFR2 (Fig. 2).

All these markers except sIL-6Rα, OCLN, CP, STAT1 and STAT3, are upregulated in tumor samples compared to controls. The log-transformed concentrations which were not normally distributed and exhibited no difference were those of Pentatrexi3 and that of sCD163.

Correlation Matrix

A new set of variables has been defined as the ratio between the biomarker levels in tumors and in control samples. Correlations between sample levels and ratios were gathered into a combined multi-type variables correlation matrix (see Fig. 3). This matrix has been compiled by reporting the highest values and highest significance levels of the correlation coefficients as follows: log-transformed levels ratios which were normally distributed are represented by Pearson correlation coefficients, the untransformed level ratios are represented by Spearman coefficients, the log-transformed tumor levels which are normally distributed are represented by Pearson coefficients, and untransformed tumor levels are represented by Spearman coefficients.

We note 5 positive correlation coefficients greater than 0.751: MMP2-IL8 (concentrations ratios in log scale) = 0.884** (Pearson), BAFF-IL8 (concentrations in tumors) = 0.820** (Spearman), IL20-IL22 (concentrations ratios in log scale) = 0.833** (Pearson), IL34-IL35 (concentration ratios in log scale) = 0.792** (Spearman) and IL6Rα-IL1Ra (concentrations in tumors) = 0.772** (Spearman).

Also, we note also the strongest 5 negative correlations (less than − 0.650): APRIL – MMP2 (concentration ratios in log scale) = − 0.761 (Pearson), APRIL-BAFF (concentrations in log scale) = − 0.740** (Pearson), APRIL-IL8 (concentrations ratios in log scale) = − 0.696** (Pearson), MMP3-LIGHT/ TNFSF14 (concentrations in tumor) = -0.684** (Spearman) and APRIL-sTNFR1 (concentrations in tumor) = − 0.667** (Spearman).

Discussion

Underexpressed and low level cytokines

An important number of cytokine levels were below the detection limit of the method (LOD and/or LLOQ) such as IL-2, IL-10, IL-11, IL-12 (p40), IL-12 (p70), IL-19, IL-27 (p28), IL-28A / IFN-λ2, IL-29/IFN-λ1, IFN-α2 in both tumor and normal tissue control samples while some other molecules (IL-12, sCD163 and sCD30) exhibited no differences in tumor and control samples. Most of these cytokines were previously reported as participants in the regulation of the anti-tumor immune response. These findings might suggest the existence of a pro-malignant phenotype in these CRC patients. Another explanation for such downregulation is that these cytokines are active during very early stages of tumor formation. This group of cytokines deserves more attention in the future because it might reveal after further analysis, potent biomarkers of early stage tumor detection. For example, IL-27, whose concentrations were below our methods detection limits, has a potent antitumor activity, related not only to the induction of tumor-specific Th1 and cytotoxic T lymphocyte responses but also to direct inhibitory effects on tumor cell

proliferation, survival, invasiveness, and angiogenic potential [14]. In addition, IL-27 together with IL-12 (another undetectable marker in our samples) mediates the activation of both STAT1 and STAT3 and also it can enhance CD4 + T cell proliferation, Th1 cell differentiation, and IFN-γ production [14]. Moreover, IFN-*γ* production was low in both normal and tumor tissue (Supplementary Table 1) and STAT1 and STAT3 were downregulated in tumor versus normal tissue (Fig. 2n and 2o). Hence, IL-27 and his co-enhancing partner IL-12 do not act in the stages were neoplastic tissue is well differentiated into a tumor, as it is in the case of our cohort formed by patients with tumors beyond the IIA stage.

Both IFN-α and IFN-β, together with IL-28 have been reported to have potent antitumor activity and are currently used in the clinical treatments of several malignancies [15]. Our results show that IFN-α and IL-28 are poorly expressed and IFN-β is significantly downregulated in tumors compare to controls (Fig. 1c).

Our results show that CD163 expression level in tumors is not statistically different from in the one in control samples. It has been previously reported [4] that the CD163 expression levels were significantly lower on monocytes from CRC patients compared to healthy donors, suggesting that colorectal tumors influence the monocytes phenotype. The mechanism behind the phenotypic regulation of monocytes and other circulating innate immune cells, such as natural killer and natural killer T cells, are not fully understood, but immunosuppressive cytokines are thought to play a major role, along with the hypoxic conditions generated in the tumor microenvironment [16].

Finally, we emphasize the low IL-2 levels in our samples. The antitumor effect of high-dose IL2 therapy was demonstrated more than three decades ago [17]. Now, IL2 is used in cancer immunotherapy for the expansion of immune cells such as NK cells, T-cells, NKT-cells, cytokine-induced killer cells and is also used as an adjuvant in the treatment of patients with melanoma, advanced colorectal cancer or ovarian cancer with autologous dendritic cells stimulated by autologous tumor lysate [6]. The efficacy of these therapies is easy to understand as the suppressed IL-2 levels are a barrier in cellular immune response.

CHI3L1-related pathways

CHI3L1 has been proposed as both a biomarker and potential therapeutic target in gastric and colorectal cancer, being overexpressed in both serum and tumor tissue [18–21] being involved in promoting cancer cell proliferation, invasion and metastasis[22]. As shown in Fig. 2a, the protein expression levels in cancer tissues were significantly higher than in adjacent normal tissues of the same patients ($p < 0.001$). Our results are in accordance with the CHI3L1 plasma levels observed in CCR patients *vs.* control and mRNA expression levels detected by Kawada et al. in colorectal cancer tissue versus normal tissues [18]. In addition, their results revealed that a strong CHI3L1 expression was significantly correlated with T stage, lymphatic invasion, vascular invasion and lymph node metastasis and the *in vitro* studies on SW480 cells indicate that CHI3L1 overexpression induces IL-8 secretion and up-regulation of Erk and JNK pathway [18]. In our cohort, immunoblot analysis of pErk1/2 (Fig. 1j) revealed that this pathway is active, the pErk1/2 levels were significantly increased in tumor tissue compared to control ($p < 0.001$). Moreover, the MMP-2 and IL-8 levels (Fig. 1g and Fig. 2c) were significantly higher in tumor tissue vs. control ($p < 0.001$). Our

results showed a significant Pearson correlation coefficient between CHI3L1 and pERk (0.43) on the one hand and on the other hand between CHI3L1 and MMP2 (0.503) (Figs. 3 and 4). Also, a strong Pearson correlation coefficient (0.59) was found between CHI3L1 and IL8 (Figs. 3 and 4). The CHI3L1 - Erk correlation is in agreement with the previously proposed mechanisms involved in tumor biology. Thus, CHI3L1 binding to CD44v3 induced the activation of Erk, Akt, and β-catenin signaling pathway enhancing cancer metastasis [23]. In cell lines, CHI3L1 stimulation results in the phosphorylation of Erk1/2 [24] and a recombinant CHI3L1 was reported to significantly enhance the proliferation of SW480 cells, through the activation of MAPK/Erk signaling pathway [25]. Overall, CHI3L1-induced MMP2 overexpressionplays a crucial role in ECM regulation promoting cancer cell growth, proliferation, invasion, and metastasis [25]. The CHI3L1, MMP2, and IL8 form a triad (Fig. 4) based on the correlation matrix (Fig. 3), which seems to play a central role in tumor local and distal development.

Another important triad correlation (Fig. 4) revealed the link between the upregulation of pErk (Fig. 1a) and CHI3L1 (Fig. 2a) and the downregulation of OCLN (Fig. 2m). The possible involvement of the Ras-Raf-MEK-ERK signaling module in regulating OCLN expression was examined in Pa-4 cells transiently transfected with either an oncogenic K-RAS, an active mutant of Raf-1, Raf BXB or with constitutively active MEK1, pFC-MEK1. In all three transfected cell, northern blots revealed the decreases OCLN mRNA levels. In addition, downregulation of OCLN expression induced by pFC-MEK1 was blocked by PD98059, a selective inhibitor of Erk activation. Furthermore in A549 cell model, with a high Ras-Raf signaling activity due to an oncogenic K-ras mutation, an upregulation of OCLN was demonstrated by transfecting a dominant negative Raf-1 construct or by treating the cells with PD98059 [26]. These results are in agreement with our study showing that elevated pErk levels are inversely correlated with OCLN protein expression (Pearson correlation − 0.54; $p < 0.01$), reinforcing that the decrease in OCLN is due to the activation of the Erk signaling pathway. Moreover, 45% of patients were diagnosed with K-RAS mutation (data not shown). In addition, a Pearson correlation coefficient (-0.49) was determined between CHI3L1 and OCLN (Fig. 3).

IL-8 an important cross-link point in cytokines constellation

We emphasize the fact that in our tumor samples IL-8 cytokine had the highest levels vs. controls (4 fold increase, Fig. 2c, Supplementary Table 1). Our study showed that this highly expressed biomarker is a member of a highlighted correlation triad formed by IL-8, IL-β1 and MMP-2 with Pearson correlation coefficients of 0.56, 0.48 and 0.88 respectively (Figs. 3 and 4). In agreement with the IL-8 and MPP2 positive correlation revealed by our data, Pengjun et al. (2013) showed that compared with the healthy controls, the colorectal adenoma patients exhibited a concomitant increase of IL-8 and MMP-2 [27]. Consecutively, the importance of MMP-2 was demonstrated by Groblewska et al. (2014) who showed that positive tissue expression of MMP-2 was a significant prognostic factor for CRC patients survival being involved in the invasion and metastasis of CRC [28].

An important implication in EMT was also revealed by IL-22 in relation with IL-1β [29], which was shown to be critically involved in CRC cell metastasis[30] We showed an important correlation between IL-8, IL-1β, MMP-2 and IL-22 (Fig. 3 and Fig. 4). IL-22 has tumor-promoting properties, enhances tumor-cell proliferation, protects against apoptosis, and mediates the attraction of immunosuppressive immune cells and the release of other pro- and anti-inflammatory cytokines [31]. In addition, cancer cells induce IL-22 production by memory CD4 + T cells via IL-1β in order to promote tumor growth [32].

A study of the immune condition of CRC patients [1] has suggested a direct relation between IL-8 and CA19-9 on one hand and IL-8 and CEA on the other hand. Our study suggests that such relation might develop through intermediary correlations such as IL8 – IL22 – CA19-9 and IL8 – IL1 β – CEA, respectively (see Fig. 4).

As discussed above, β-catenin pathway activation through IL-8 induces EMT and the increases of MMP-2 expression and activity [33]. We found a downregulation of IFN-β in tumor tissue compared to control (Fig. 1c) and a negative Pearson correlation with MMP-2 (-0.501). Moreover, in CRC it was demonstrated that β-catenin could inhibit the expression of IFN-β and interferon-stimulated gene 56 (ISG56) by interacting with the central transcription factor, interferon-regulatory factor 3 and blocking its nuclear translocation, responsible for the induction of IFN-β and being hence essential for the activation of interferon responses [34]. This result might be relevant for immunotherapy development because it has recently been shown that IFN-β can sensitize CRC cells to 5-fluorouracyl treatment with a potent effect on the reduction of tumor mass, suggesting a novel strategy to selectively target CRC [35].

APRIL, BAFF, IL-8 and MMP-2 cluster as potential therapeutic targets

Only scarce data exist about APRIL and BAFF roles in CRC tumor biology. The breast cancer is one of the few solid tumors described by a differential role of BAFF and APRIL, produced in important quantities either by stromal cells or infiltrating neutrophils [36]. BAFF is constantly present in both normal and tumor tissue, while APRIL is preferentially expressed by the non-cancerous breast epithelial tissue, while its expression was shown to be decreased in breast tumor cells. In addition, APRIL expression was inversely correlated with the tumor stage of breast cancers [36,37].

Recently the possible role of APRIL–BAFF and of their receptors in solid tumors has been studied by using Oncomine resources to investigate The Cancer Genome Atlas (TCGA) in order to compare tumor vs. normal mRNA expression in the whole spectrum of the samples' collection [35]. All the tumor samples analyzed exhibited APRIL and BAFF expression, together with those of their receptors. APRIL and BRAF were usually downregulated in tumors as compared to normal control. CRC was the only exception from this rule: BRAF is upregulated in tumor samples as compared to their non- counterparts [37]. In that study data from over 881 CRC tissue samples were analysed and their reports are in correlation with our results that found one of the strongest negative Pearson correlation between APRIL and BAFF (− 0.740). Additionally, our results also showed strong $p < 0.001$ correlation between BAFF and IL8 (0.820,

Spearman), APRIL and BAFF (-0.740, Pearson), APRIL and IL8 (− 0.696, Pearson), APRIL and MMP2 (-0.761, Pearson), MMP2 and IL8 (0.884, Pearson).

The STAT 1 and STAT3 downregulation plays a role in tumor growth

The STAT1 and STAT3 transcription factors have been identified as major players in tumor genesis and they are being considered promising target proteins for cancer therapy. They are thought to play opposite roles, namely, STAT1 is involved in activating immunosurveillence and it is considered a tumor suppressor [38], while STAT 3 is considered an oncogene, and its persistent signaling contributes to stimulate cell proliferation and prevent apoptosis[2]. STAT1 inhibition was reported in diverse tumor types, along with overexpressed STAT3[39]. However, the role of STAT3 in CRC development remains controversial, as there are reports either elevated tumor promoting STAT3 activity but also STAT3-related tumor inhibitory [40]. Interestingly, more recently, concomitant absence of STAT1 and STAT3 was reported in CRC tumor tissue, which was found to be significantly correlated with shorter overall survival of CRC patients [40]. *In vitro* experiments on various colon cancer cell lines revealed that STAT3 activity is subjected to particular changes in the inflammatory tumor microenvironment [41], most notably IL6 high levels stimulate STAT3.

In vitro functional studies revealed that IL6 utilizes the GP130/IL6 hexameric signaling complex, which includes IL6Rα [42], a receptor chain component which is typically upregulated in cancer cell lines. Here we report, both diminished levels of STAT1 and STAT3 in CRC as compared to non-transformed colon tissue, but also reduced IL6Rα, which may contribute to explain this phenomenon. Interestingly, recent developments of therapeutic approaches are considering the pharmacological blockage of STAT3 signaling [42], however, given our findings of already reduced STAT1 and 3 in CRC tumors and also the association of low STAT1 concomitant with STAT3 with reduced survival of CRC patients [40], great caution should be considered when designing such therapies.

Finally, in the series of down regulated biomarkers related to STAT1 and STAT3, we mention TWEAK. In CRC patients, increased tumor levels of TWEAK were found to be associated with statistically significantly higher overall survival [43]. *In vitro* invasion assays revealed TWEAK displays an inverse relation with tumor invasive ability. Our study reveals significantly reduced TWEAK in tumor samples, which is negatively correlated in tumor tissues with MMP1 and MMP3 (Fig. 3 and Fig. 4).

This study is a systematic investigation of a wide range of inflammatory factors involved in colon cancer related signaling pathways. We report the existence of a panel of underexpressed markers (namely IL-2, IL-10, IL-11, IL-12 (p40), IL-12 (p70), IL-19, IL-27 (p28), IL-28A / IFN-λ2, IL-29/IFN-λ1, IFN-α2) in CRC patients, which should be further studied to reveal their role in establishing a pro-tumoral inflammatory conditions. Our results bring into focus an often overlooked association of markers which might be specific to colon cancer tumors, namely diminished APRIL levels and high BAFF, as opposed to other tumor types which display both APRIL and BRAF downregulated levels. Together with IL-8 and MMP2,

these two markers show strong correlation. This biomarker panel supports a possible combined target immunotherapy approach in colon cancer treatment.

Methods

Study design

This study was performed in accordance with the Declaration of Helsinki 1975, amended in 2013. All protocols and methods carried out were review and approved by the Medical Ethics Committee of Elias University Emergency Hospital in Bucharest (no: 5939 / 2019). Prior to being included in the study, written informed consents have been signed by all participant patients.

Our patient cohort included 28 patients who underwent surgery in order to remove colorectal tumors at Elias University Emergency Hospital between January 2019 and May 2020. However, 6 of these patients have tested positive for SARS-CoV2, the day after surgery. Since at biological level, the inflammatory profile of these patients might have been influenced by this viral infection known to trigger the so-called „cytokine storm”[44] these 6 patients have been excluded from the study. The remaining N = 22 patients have been included in the study and submitted to the study protocol described below.

In Table 1 we present the demographic and clinical data of our study cohort. The cohort is formed 54.5% (12) male and 45.5 (10) female subjects. Body Mass Index (BMI) of the whole cohort has been categorized according to the World Health Organization classification of obesity [45]. Although both obesity and CRC incidence rates are increasing, it is yet unclear what relationship, if any, exists between BMI, cancer recurrence and patient survival[46]. We have defined the following categories of tumor localization according to the colorectal anatomic segments: proximal region and distal region.

Table 1
Clinical, demographic and staging data of the study cohort.

Variable	Mean	Median	SD.	Min.	Max.
Age (years)	66.14	64.50	9.285	50	81
Female	64.90	64.00	8.412	50	81
Male	67.17	66.50	10.205	52	81
BMI (kg/m^2)	27.19	26.57	4.426	20	41
Female	28.36	27.08	5.644	20	41
Male	26.22	26.40	3.011	22	32
Variable	**Category**			**Value**	**%**
Gender	Female			10	45.5
	Male			12	54.5
BMI (kg/m^2)	Underweight (< 18.5)			0	0
	Normal range (18.5 to 24.9)			8	36.4
	Overweight (≥ 25)			14	73.6
	Pre-obese (25.0 to 29.9)			10	45.4
	Obese class 1 (30.0 to 34.9)			3	13.7
	Obese class 2 (30.0 to 34.9)			0	0
	Obese class 3 (≥ 40)			1	4.5
Smoking habits	**Smokers**			**5**	**22.7**
	Female			1	4.5
	Male			4	18.2
	Non-Smokers			**17**	**77.3**
	Female			11	50.0
	Male			6	27.3
Arterial Hypertension	Optimal (TAs < 120 and TAd < 80)			2	9.2
	Normal (TAs = 120–129 and/or TAd = 80–84)			14	63.6
	High Normal (TAs = 130–139 and/or TAd = 85–89)			5	22.7
	Grade 1 (TAs = 140–149 and/or TAd = 90–99)			1	4.5

Variable	Mean	Median	SD.	Min.	Max.
Staging	I			2	9.1
	IIA			6	27.3
	IIB			2	9.1
	IIIB			3	13.6
	IIIC			3	13.6
	IVA			6	27.3

Within this definition 40.9% of patients (9) were subjected to surgery concerning tumors situated in the distal region and 59.1% of patients (13) were subjected to surgery concerning tumors situated in the proximal region.

Prior to the surgery the patients have been submitted to standard arterial tension measurements. The mean valued allowed the classification of these patients according to the European Society of Cardiology (ESC) and to the European Society for Hypertension (ESH) criteria [47] in optimal, normal, high normal blood pressure (BP) and grade 1–3 hypertension. Table 1 shows that most of the patients 72.7% (16) had optimal or normal BP while 27.2% (6) of them were in the early stages of arterial hypertension (high normal BP and grade 1 stages).

The cancer staging in Table 1 has been established using the ypTNM classification of tumors from histopatological samples by AJCC classification criteria grid [48].

Tissue samples and lysates preparation

This study utilized tumor and paired normal tissue samples available from 22 of the patients who underwent surgery in order to remove colorectal tumors. Tumor tissue and adjacent normal mucosa from each patient were excised and immediately frozen at − 80 °C until analysis. Frozen tumor and paired normal tissue (100 mg) were thawed and homogenized in ice cold cell lysis buffer (provided by Bio-Plex Pro cell signaling kit, Bio-Rad Laboratories, Hercules, CA, USA) containing a protease inhibitor cocktail using ceramic beads and TeSeE PRECESS 24 Homogenizer (Bio-Rad Laboratories, Hercules, CA, USA) according to the manufacturer's instructions. The lysate was placed on ice for 10 min and then centrifuged at 14,000 × g for 10 min. The protein content of the supernatant was determined for each sample using the Pierce Rapid Gold BCA Protein Assay Kit (Thermo Fisher Scientific, MA, USA). Finally, the supernatant was aliquoted and frozen at − 80 ºC, for subsequent biochemical and immunochemical analyses.

Biomarkers quantization

Inflammatory cytokines and MMPs

Supernatant samples with a total protein concentration of 900 µg/mL were used for the detection of APRIL / TNFSF13, BAFF / TNFSF13B, sCD30 / TNFRSF8, sCD163, CHI3L1, gp130 / sIL-6Rβ, IFN-α2, IFN-β, IFN-γ, IL-2, sIL-6Rα, IL-8, IL-10, IL-11, IL-12 (p40), IL-12 (p70), IL-19, IL-20, IL-22, IL-26, IL-27 (p28), IL-28A / IFN-λ2, IL-29/IFN-λ1, IL-32, IL-34, IL-35, LIGHT / TNFSF14, MMP-1, MMP-2, MMP-3, Osteocalcin, Osteopontin, Pentraxin-3, sTNF-R1, sTNF-R2, TSLP and TWEAK / TNFSF12 biomarkers using the Bio-Plex Pro Human Inflammation 37-plex Panel1 (Bio-Rad Laboratories, Hercules, CA, USA). The IL-1β and IL-1Ra was quantified separately using the Bio-Plex Pro Human Cytokine Standard 27-plex, Group I, magnetic beads and detection antibodies for human IL-1β and IL-1Ra (Bio-Rad Laboratories, Hercules, CA, USA). The biomarker levels were analyzed according to manufacturer's instructions, using the Bio-Plex MAGPIX System and Bio-Plex Manager software version 6.0 (Bio-Rad Laboratories, Hercules, CA, USA) as previously described[49,50].

ELISA assay for CEA and CA19-9

CEA and CA19-9 levels from tissue lysates were quantified by using CanAg CEA EIA kit (Fujirebio Diagnostics AB, Sweden) and CanAg CA19-9 EIA 120 – 10 (Fujirebio Diagnostics AB, Sweden), according to the manufacturer's protocol. The protein concentration of the tissue lysate for CEA assay was 1.5 mg/mL and for CA19-9 assay was 75 µg/mL.

Western Blot assays

For target protein expression evaluation, protein tissue lysates were resolved on Protean TGX Stain Free 4%–20% precast gels (Bio-Rad Laboratories, Hercules, CA, USA), transferred onto 2 µm nitrocellulose membrane (V3 Western Workflow, Bio-Rad Laboratories, Hercules, CA, USA) and total protein transferred signal was detected and quantified using the ChemiDoc MP System and Image Lab software (version 5.2.1, Bio-Rad Laboratories, Hercules, CA, USA). The membranes were blocked using EveryBlot Blocking Buffer for 5 min at room temperature. Mouse anti-human ERK/MAPK (pThr202/pTyr204) monoclonal antibody (MCA5990GA, 1:1000 dilution factor), mouse anti-human OCLN monoclonal antibody (MCA3308Z, 1:250 dilution factor), mouse anti-human STAT1 monoclonal antibody (MCA3469Z, 1:350 dilution factor) and goat anti-human STAT3 polyclonal antibody (AHP1076, 1:500 dilution factor), were used. HRP conjugated secondary antibodies (STAR 120 and STAR 122 at 1:500 and 1:15.000 dilution factor respectively, Bio-Rad antibodies, Hercules, CA, USA) were used. For immunostaining of the membranes, they were incubated with the primary antibodies for 2 h and with the secondary antibodies for 1 h at room temperature, under constant homogenization. Blots were revealed using the Clarity Western ECL Substrate (Bio-Rad Laboratories, Hercules, CA, USA) and the chemiluminescence signal was detected using the ChemiDoc MP System. The target proteins expression was quantified using the Image Lab software version 5.2.1 (Bio-Rad Laboratories, Hercules, CA, USA), and normalized to the total proteins transferred onto the membrane (each protein band was normalized against the total proteins transferred in the corresponding lane)[51].

Cellular carbonylated protein detection was performed using the OxiSelect Protein Carbonyl Immunoblot Kit (Cell Biolabs, San Diego, CA, USA) with a post-transfer derivatization step of protein-bound carbonyl

groups by treatment with a solution of dinitrophenylhydrazine (DNPH). The formed adducts were recognized by a primary rabbit anti-DNPH (diluted 1:1000), and HRP conjugated secondary antibody anti-rabbit IgG (diluted 1:1000) as previously described [49].

Statistical analysis

Preliminary data validation

The biomarkers levels were analysis with Bio-Plex Manager software version 6.0 (Bio-Rad Laboratories, Hercules, CA, USA). The coefficient of variation (COV), percentage recovery and normality distribution of data have been checked before proceeding to the statistical analysis. Data distribution for sample replicates has been assessed using the COV for assay whose limits are 15% (intra-assay precision) and 20% (inter-assay precision).

To ensure the data reliability quality controls have been run in parallel to the Bio-Plex sample assay. These controls are in fact samples containing analytes in known concentration provided by the assay manufacturer. Percentage recovery of 80–120% is considered acceptable to support accurate sample interpretation.

Statistical Analysis Steps

After the validation of the COV and of the percentage step, statistical analysis has been performed as follows: normality checks, log transformations for data normalization, comparisons control vs. tumor samples and correlations. Data analysis has been performed using the IBM SPSS Statistics 26 statistical analysis package.

Our first objective is to assess the statistically significant differences for all markers in control vs. tumor samples by applying the corresponding tests. The first step in choosing the comparison test is to check the normality distribution of the raw concentration and densitometry data.

A Shapiro-Wilks test($p > 0.05$) and a visual inspection of their histograms, normal Q-Q plots and box plots have been used at this stage to check the normality distribution for each biomarker concentrations data for both control and tumor sample. Within this Shapiro-Wilks test the null hypothesis is the normal distribution of data. This hypothesis is rejected for $p < 0.05$ and it is accepted for $p > 0.05$.

Data sets failing the initial normality test i.e. for which $p < 0.05$, have been normalized through log transformation i.e. $y \rightarrow \log(y)$. The newly obtained data sets have been again submitted to the Shapiro-Wilks normality test.

Our samples were paired-related samples being collected from the same patients according to the above described protocol. The normally distributed data sets have been submitted to parametric means comparison testing (t-Student tests, see Fig. 1) and the data sets which were not normalized post log transformation have been submitted to non-parametric comparison testing (Wilcoxon, see Fig. 2). The

biomarkers concentrations have been considered different if $p < 0.05$. The biomarkers failing the comparison tests have been excluded.

For the purpose of correlation, a new set of variables have been defined as the ratio between the biomarker level in tumor and that in control. The levels ratios normal distribution has been checked by Shapiro-Wilks testing. The ratios failing the first stage normality testing have been log-transformed and the Shapiro-Wilks test has been applied again.

Log-transformed variables and ratios that are normally distributed have been included in Pearson correlation matrices, while the remaining variables and the ratios which were not normally distributed have been included in Spearman correlation matrices. Since all the untransformed variables and ratios were not normally distributed the Spearman correlation coefficients have been also calculated for both tumor related data and ratios.

The correlation coefficients represent a measure of a monotonic relation between the paired data. The nearer this coefficient is to ± 1 the stronger the monotonic relationship is. If the correlation is significant at a 0.01 level (2-tailed) the coefficient value is marked by two stars (**) and if this correlation is significant at a 0.05 level the coefficient value is marked by a star (*).

All the correlation matrices between untransformed tumor related data, log-transformed normally distributed variables, log transformed normally distributed ratios and the untransformed ratios have been combined into a combined multi-type variables correlation matrix (see Fig. 3). The correlation coefficients have been colored specifically to identify their origin and a hierarchy has been established according to the following criteria (1) Pearson correlations were considered stronger than Spearman correlations, (2) 0.01 (2 tailed) coefficients are more stronger than the 0.05 (2 tailed) coefficients and (3) ratios related correlations were considered stronger than untransformed simple variable correlations.

Declarations

Acknowledgements

This work was supported by a grant of the Romanian Ministry of Education and Research, CCCDI – UEFISCDI project number PN-III-P2-2.1-PTE-2019-0544, within PNCDI III. The funders had no role in the study design, data collection and analysis, decision to publish or preparation of the manuscript.

Author contributions

V.C. and A.I. had equal contributions to this work. V.C., A.I. and A.I.S. conceived and designed the study. V.C., A.I.S., L.S., F.I., O.I.G., A.I. and A.M.P. performed the experiments and acquired the data. V.C., A.I.S., L.S., F.I., O.I.G., A.I., A.M.P., and LB analyzed and interpreted the data. LS and LB prepared figures. LB performed the statistical analysis. V.C., L.S., F.I., O.I.G., A.I., and A.M.P. drafted the manuscript. A.I.S. and

LB write and review the manuscript. A.I.S. supervised all experimental procedures. V.C. and A.I.S. were involved in funding acquisition. All authors reviewed and approved the manuscript.

Competing interests:

The authors declare no competing financial and non-financial interests.

Corresponding author

Please address correspondence to Andreea Iren Serban (email: irensro@yahoo.com).

References

1. Komura, T., *et al.* Immune Condition of Colorectal Cancer Patients Featured by Serum Chemokines and Gene Expressions of CD4 + Cells in Blood. *Canadian Journal of Gastroenterology and Hepatology* **2018**, 7436205 (2018).
2. Corvinus, F.M., *et al.* Persistent STAT3 activation in colon cancer is associated with enhanced cell proliferation and tumor growth. *Neoplasia* **7**, 545–555 (2005).
3. Klampfer, L. Cytokines, inflammation and colon cancer. *Curr Cancer Drug Targets* **11**, 451–464 (2011).
4. Coussens, L.M. & Werb, Z. Inflammation and cancer. *Nature* **420**, 860–867 (2002).
5. Nogueira-Costa, G., *et al.* Prognostic utility of neutrophil-to-lymphocyte ratio in patients with metastatic colorectal cancer treated using different modalities. *Curr Oncol* **27**, 237–243 (2020).
6. Chulpanova, D.S., Kitaeva, K.V., Green, A.R., Rizvanov, A.A. & Solovyeva, V.V. Molecular Aspects and Future Perspectives of Cytokine-Based Anti-cancer Immunotherapy. *Front Cell Dev Biol* **8**, 402–402 (2020).
7. West, N.R., McCuaig, S., Franchini, F. & Powrie, F. Emerging cytokine networks in colorectal cancer. *Nat. Rev. Immunol.* **15**, 615–629 (2015).
8. Vainer, N., Dehlendorff, C. & Johansen, J.S. Systematic literature review of IL-6 as a biomarker or treatment target in patients with gastric, bile duct, pancreatic and colorectal cancer. *Oncotarget* **9**, 29820–29841 (2018).
9. Xu, J., *et al.* Diagnostic and Prognostic Value of Serum Interleukin-6 in Colorectal Cancer. *Medicine (Baltimore)* **95**, e2502-e2502 (2016).
10. Akhmaltdinova, L., *et al.* Inflammatory Serum Biomarkers in Colorectal Cancer in Kazakhstan Population. *International Journal of Inflammation* **2020**, 9476326 (2020).
11. Bhardwaj, M., *et al.* Multiplex screening of 275 plasma protein biomarkers to identify a signature for early detection of colorectal cancer. *Molecular Oncology* **14**, 8–21 (2020).
12. Nikolaou, S., *et al.* Systematic review of blood diagnostic markers in colorectal cancer. *Techniques in Coloproctology* **22**, 481–498 (2018).

13. Annaházi, A., *et al.* A pilot study on faecal MMP-9: a new noninvasive diagnostic marker of colorectal cancer. *Br J Cancer* **114**, 787–792 (2016).
14. Fabbi, M., Carbotti, G. & Ferrini, S. Dual Roles of IL-27 in Cancer Biology and Immunotherapy. *Mediators Inflamm* **2017**, 3958069–3958069 (2017).
15. Numasaki, M., *et al.* IL-28 Elicits Antitumor Responses against Murine Fibrosarcoma. *The Journal of Immunology* **178**, 5086–5098 (2007).
16. Krijgsman, D., *et al.* CD163 as a Biomarker in Colorectal Cancer: The Expression on Circulating Monocytes and Tumor-Associated Macrophages, and the Soluble Form in the Blood. *Int. J. Mol. Sci.* **21**, 5925 (2020).
17. West, W.H. Continuous infusion recombinant interleukin-2 (rIL-2) in adoptive cellular therapy of renal carcinoma and other malignancies. *Cancer Treat Rev.* **16**, 83–89 (1989).
18. Kawada, M., *et al.* Chitinase 3-like 1 promotes macrophage recruitment and angiogenesis in colorectal cancer. *Oncogene* **31**, 3111–3123 (2012).
19. Faibish, M., Francescone, R., Bentley, B., Yan, W. & Shao, R. A YKL-40-neutralizing antibody blocks tumor angiogenesis and progression: a potential therapeutic agent in cancers. *Mol Cancer Ther* **10**, 742–751 (2011).
20. Johansen, J.S., *et al.* Elevated Plasma YKL-40 Predicts Increased Risk of Gastrointestinal Cancer and Decreased Survival After Any Cancer Diagnosis in the General Population. *Journal of Clinical Oncology* **27**, 572–578 (2008).
21. , *et al.* Serum YKL-40 in Risk Assessment for Colorectal Cancer: A Prospective Study of 4,496 Subjects at Risk of Colorectal Cancer. *Cancer Epidemiology Biomarkers & Prevention* **24**, 621 (2015).
22. Qiu, Q.-C., *et al.* CHI3L1 promotes tumor progression by activating TGF-β signaling pathway in hepatocellular carcinoma. *Scientific Reports* **8**, 15029–15029 (2018).
23. Geng, B., *et al.* Chitinase 3-like 1-CD44 interaction promotes metastasis and epithelial-to-mesenchymal transition through β-catenin/Erk/Akt signaling in gastric cancer. *J Exp Clin Cancer Res* **37**, 208–208 (2018).
24. Areshkov, P.O., Avdieiev, S.S., Balynska, O.V., Leroith, D. & Kavsan, V.M. Two closely related human members of chitinase-like family, CHI3L1 and CHI3L2, activate ERK1/2 in 293 and U373 cells but have the different influence on cell proliferation. *Int J Biol Sci* **8**, 39–48 (2012).
25. Zhao, T., Su, Z., Li, Y., Zhang, X. & You, Q. Chitinase-3 like-protein-1 function and its role in diseases. *Signal Transduct Target Ther* **5**, 201–201 (2020).
26. Li, D. & Mrsny, R.J. Oncogenic Raf-1 disrupts epithelial tight junctions via downregulation of occludin. *J Cell Biol* **148**, 791–800 (2000).
27. Pengjun, Z., *et al.* Multiplexed cytokine profiling of serum for detection of colorectal cancer. *Future Oncol.* **9**, 1017–1027 (2013).
28. Groblewska, M., *et al.* Serum levels and tissue expression of matrix metalloproteinase 2 (MMP-2) and tissue inhibitor of metalloproteinases 2 (TIMP-2) in colorectal cancer patients. *Tumour Biol* **35**,

3793–3802 (2014).

29. Baker, K.J., Houston, A. & Brint, E. IL-1 Family Members in Cancer; Two Sides to Every Story. *Frontiers in Immunology* **10**(2019).
30. Ieda, T., *et al.* Visualization of epithelial-mesenchymal transition in an inflammatory microenvironment-colorectal cancer network. *Scientific Reports* **9**, 16378–16378 (2019).
31. Huber, S., *et al.* IL-22BP is regulated by the inflammasome and modulates tumorigenesis in the intestine. *Nature* **491**, 259–263 (2012).
32. Voigt, C., *et al.* Cancer cells induce interleukin-22 production from memory CD4 + T cells via interleukin-1 to promote tumor growth. *Proceedings of the National Academy of Sciences* **114**, 12994 (2017).
33. Wen, J., *et al.* IL-8 promotes cell migration through regulating EMT by activating the Wnt/β-catenin pathway in ovarian cancer. *J Cell Mol Med* **24**, 1588–1598 (2020).
34. Ding, C., *et al.* β-catenin regulates IRF3-mediated innate immune signalling in colorectal cancer. *Cell Prolif* **51**, e12464-e12464 (2018).
35. Di Franco, S., Turdo, A., Todaro, M. & Stassi, G. Role of Type I and II Interferons in Colorectal Cancer and Melanoma. *Frontiers in Immunology* **8**(2017).
36. Pelekanou, V., *et al.* Expression of TNF-superfamily members BAFF and APRIL in breast cancer: immunohistochemical study in 52 invasive ductal breast carcinomas. *BMC Cancer* **8**, 76–76 (2008).
37. Kampa, M., Notas, G., Stathopoulos, E.N., Tsapis, A. & Castanas, E. The TNFSF Members APRIL and BAFF and Their Receptors TACI, BCMA, and BAFFR in Oncology, With a Special Focus in Breast Cancer. *Front Oncol* **10**, 827–827 (2020).
38. Avalle, L., Pensa, S., Regis, G., Novelli, F. & Poli, V. STAT1 and STAT3 in tumorigenesis: A matter of balance. *JAKSTAT* **1**, 65–72 (2012).
39. Buettner, R., Mora, L.B. & Jove, R. Activated STAT Signaling in Human Tumors Provides Novel Molecular Targets for Therapeutic Intervention. *Clinical Cancer Research* **8**, 945 (2002).
40. Nivarthi, H., *et al.* The ratio of STAT1 to STAT3 expression is a determinant of colorectal cancer growth. *Oncotarget; Vol 7, No 32* (2018).
41. Quante, M., Varga, J., Wang, T.C. & Greten, F.R. The gastrointestinal tumor microenvironment. *Gastroenterology* **145**, 63–78 (2013).
42. Thilakasiri, P., *et al.* Repurposing the selective estrogen receptor modulator bazedoxifene to suppress gastrointestinal cancer growth. *EMBO Molecular Medicine* **11**, e9539 (2019).
43. Lin, B.-R., *et al.* Prognostic Significance of TWEAK Expression in Colorectal Cancer and Effect of Its Inhibition on Invasion. *Annals of Surgical Oncology* **19**, 385–394 (2012).
44. Ragab, D., Salah Eldin, H., Taeimah, M., Khattab, R. & Salem, R. The COVID-19 Cytokine Storm; What We Know So Far. *Frontiers in Immunology* **11**(2020).
45. Aronne, L.J. Classification of Obesity and Assessment of Obesity-Related Health Risks. *Obesity Research* **10**, 105S-115S (2002).

46. Lee, D.-W., Cho, S., Shin, A., Han, S.-W. & Kim, T.-Y. Body mass index and body weight change during adjuvant chemotherapy in colon cancer patients: results from the AVANT trial. *Scientific Reports* **10**, 19467 (2020).
47. Williams, B., *et al.* 2018 ESC/ESH Guidelines for the management of arterial hypertension: The Task Force for the management of arterial hypertension of the European Society of Cardiology (ESC) and the European Society of Hypertension (ESH). *European Heart Journal* **39**, 3021–3104 (2018).
48. *AJCC Cancer Staging Manual*, (Springer International Publishing, 2017).
49. Geicu, O.I., *et al.* Dietary AGEs involvement in colonic inflammation and cancer: insights from an in vitro enterocyte model. *Scientific Reports* **10**, 2754 (2020).
50. Serban, A.I., Stanca, L., Geicu, O.I. & Dinischiotu, A. AGEs-Induced IL-6 Synthesis Precedes RAGE Up-Regulation in HEK 293 Cells: An Alternative Inflammatory Mechanism? *Int. J. Mol. Sci.* **16**, 20100–20117 (2015).
51. Geicu, O.I., Stanca, L., Dinischiotu, A. & Serban, A.I. Proteomic and immunochemical approaches to understanding the glycation behaviour of the casein and β-lactoglobulin fractions of flavoured drinks under UHT processing conditions. *Scientific Reports* **8**, 12869 (2018).

Figures

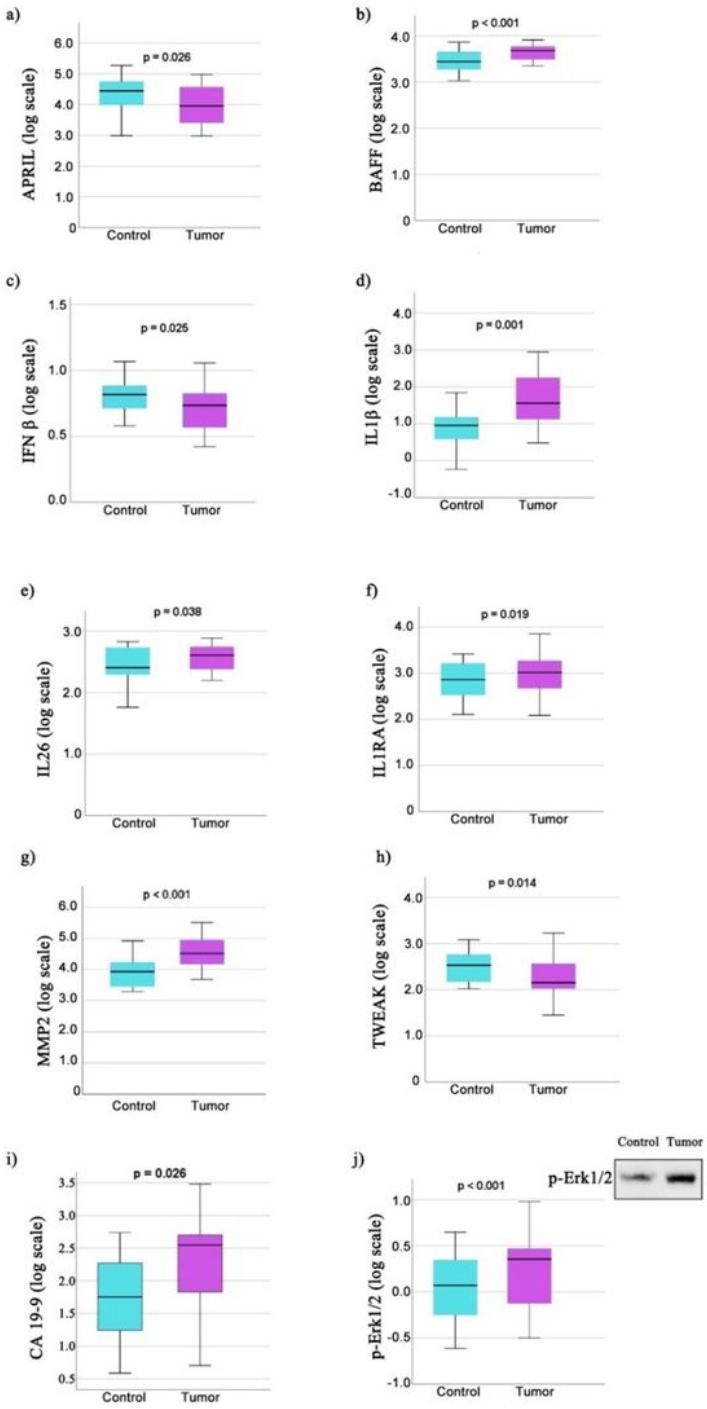

Figure 1

Boxplots of biomarkers whose log-transformed values in control and in tumor were normally distributed. a) APRIL; b) BAFF; c) IFN β; d) IL1β; e) IL26; f) IL1RA; g) MMP2; h) TWEAK; i) CA19-9; j) p-Erk1/2, also showing a cropped insert containing a representative immunoblot example. The original immunoblot image is available in Supplementary Figure S1; p-values resulting from mean comparison of control and

tumor means of log-transformed concentration values through t-Student test are written above each boxplot pair.

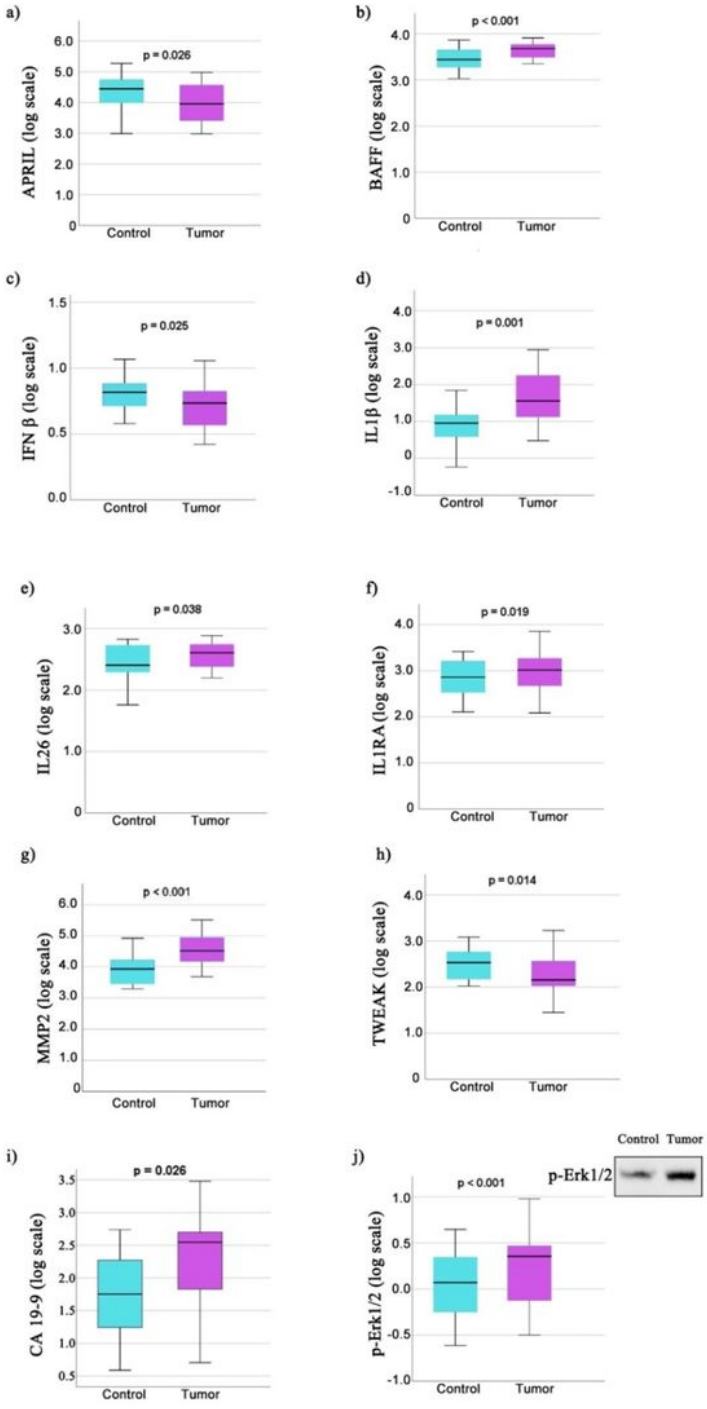

Figure 1

Boxplots of biomarkers whose log-transformed values in control and in tumor were normally distributed. a) APRIL; b) BAFF; c) IFN β; d) IL1β; e) IL26; f) IL1RA; g) MMP2; h) TWEAK; i) CA19-9; j) p-Erk1/2, also showing a cropped insert containing a representative immunoblot example. The original immunoblot

image is available in Supplementary Figure S1; p-values resulting from mean comparison of control and tumor means of log-transformed concentration values through t-Student test are written above each boxplot pair.

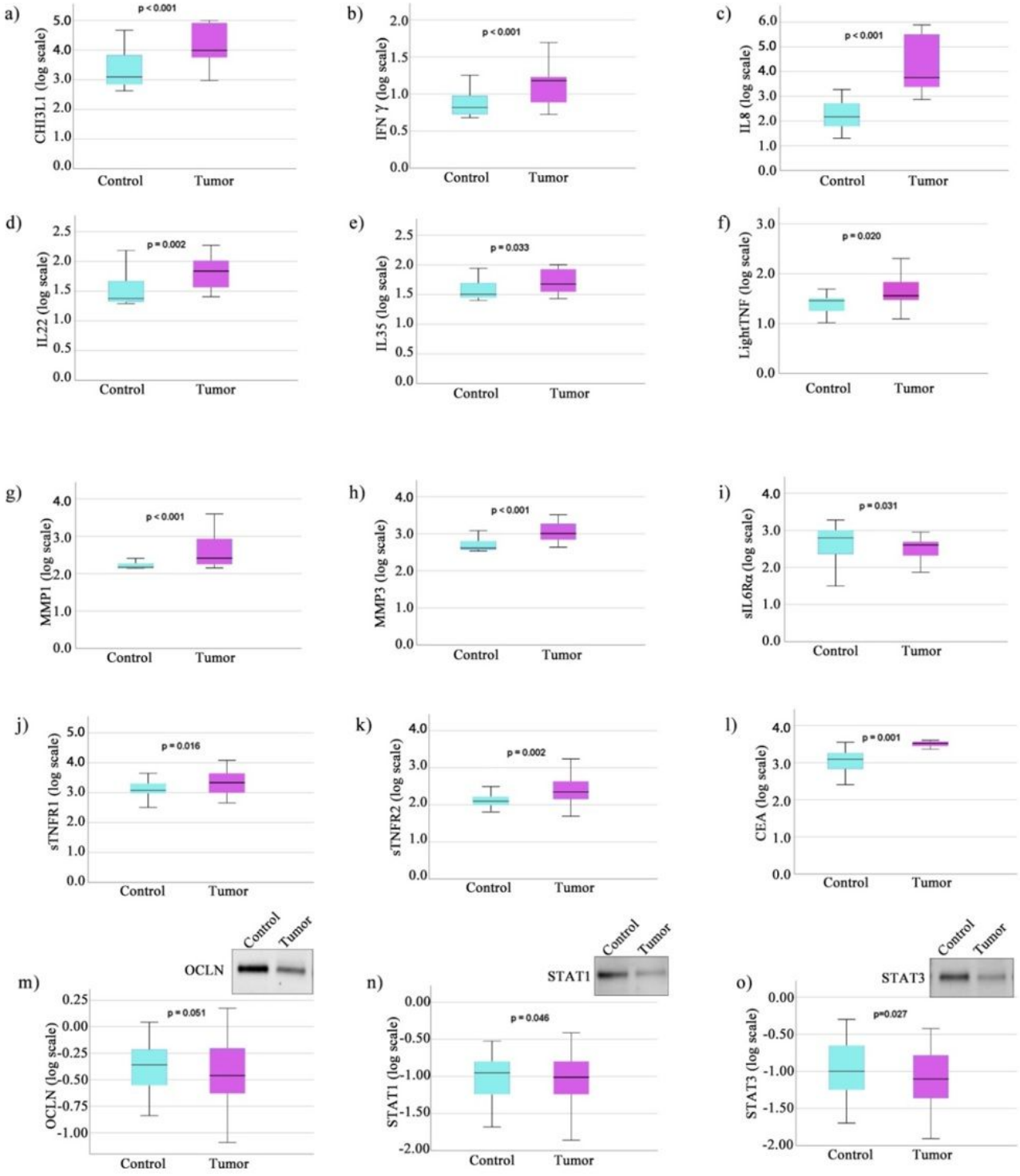

Figure 2

Boxplots of biomarkers whose log-transformed values in control and in tumor are not normally distributed. a) CHI3L1; b) IFN γ; c) IL8; d) IL22; e) IL35; f) Light TNF; g) MMP1; h) MMP3; i) sIL6Rα; j)

sTNFR1; k) sTNFR2; l) CEA; m) OCLN, also showing a cropped insert containing a representative immunoblot example (the original immunoblot image is available in Supplementary Figure S2); n) STAT1, also showing a cropped insert containing a representative immunoblot example (the original immunoblot image is available in Supplementary Figure S3); o) STAT3, also showing a cropped insert containing a representative immunoblot example. The original immunoblot image is available in Supplementary Figure S4; p-values resulting from mean comparison of control and tumor means of log-transformed concentration values through the Wilcoxon test are written above each boxplot pair.

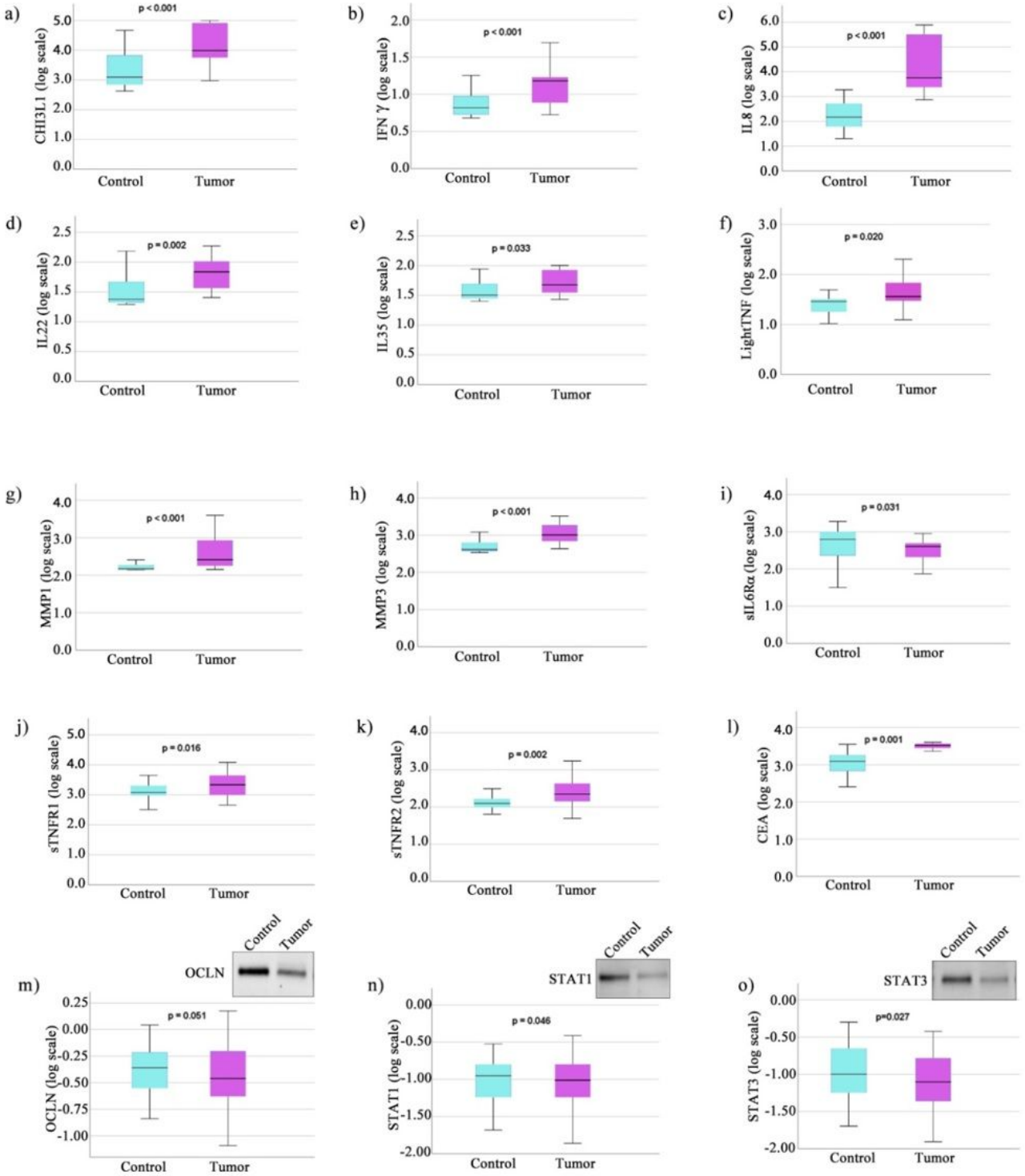

Figure 2

Boxplots of biomarkers whose log-transformed values in control and in tumor are not normally distributed. a) CHI3L1; b) IFN γ; c) IL8; d) IL22; e) IL35; f) Light TNF; g) MMP1; h) MMP3; i) sIL6Rα; j) sTNFR1; k) sTNFR2; l) CEA; m) OCLN, also showing a cropped insert containing a representative immunoblot example (the original immunoblot image is available in Supplementary Figure S2); n) STAT1, also showing a cropped insert containing a representative immunoblot example (the original immunoblot image is available in Supplementary Figure S3); o) STAT3, also showing a cropped insert containing a representative immunoblot example. The original immunoblot image is available in Supplementary Figure S4; p-values resulting from mean comparison of control and tumor means of log-transformed concentration values through the Wilcoxon test are written above each boxplot pair.

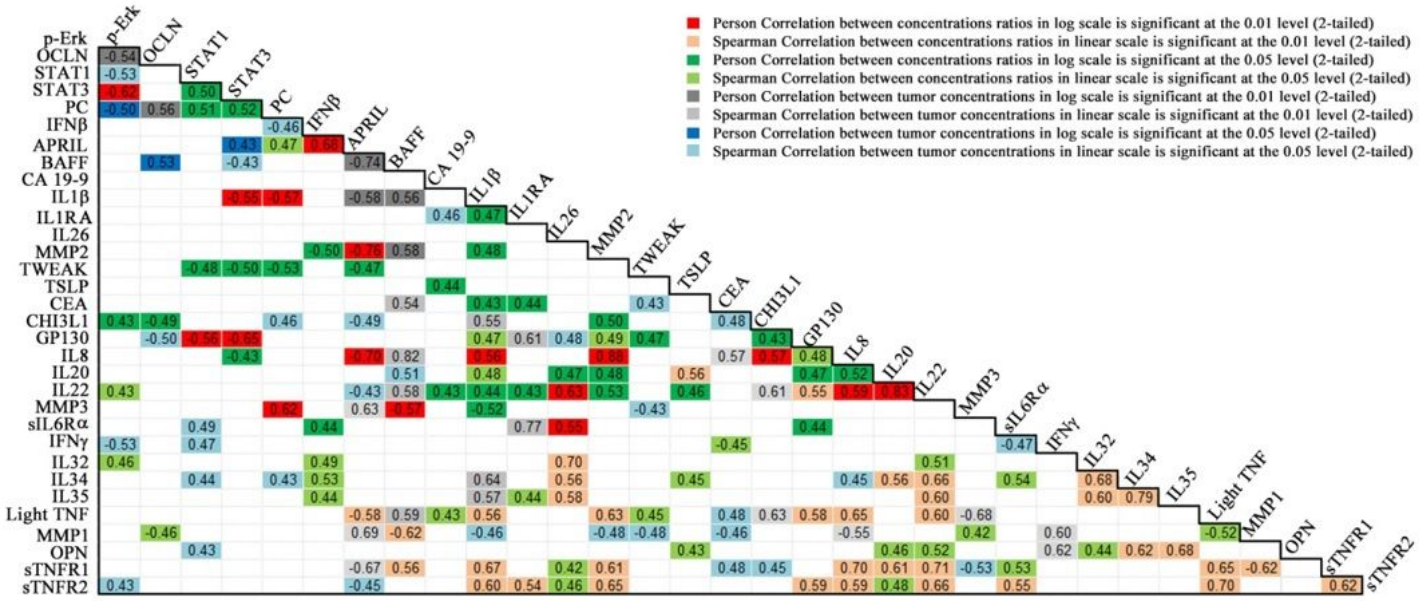

Figure 3

Combined multi-type variables correlation matrix containing the highest values of the correlation coefficients. The combinations between the two levels of significance (0.01 and 0.05) and the calculation methods (Pearson or Spearman) is color-coded, as showed by the legend in the upper-right of the matrix. See Supplementary Figure S5 for protein carbonyl immunoblot examples.

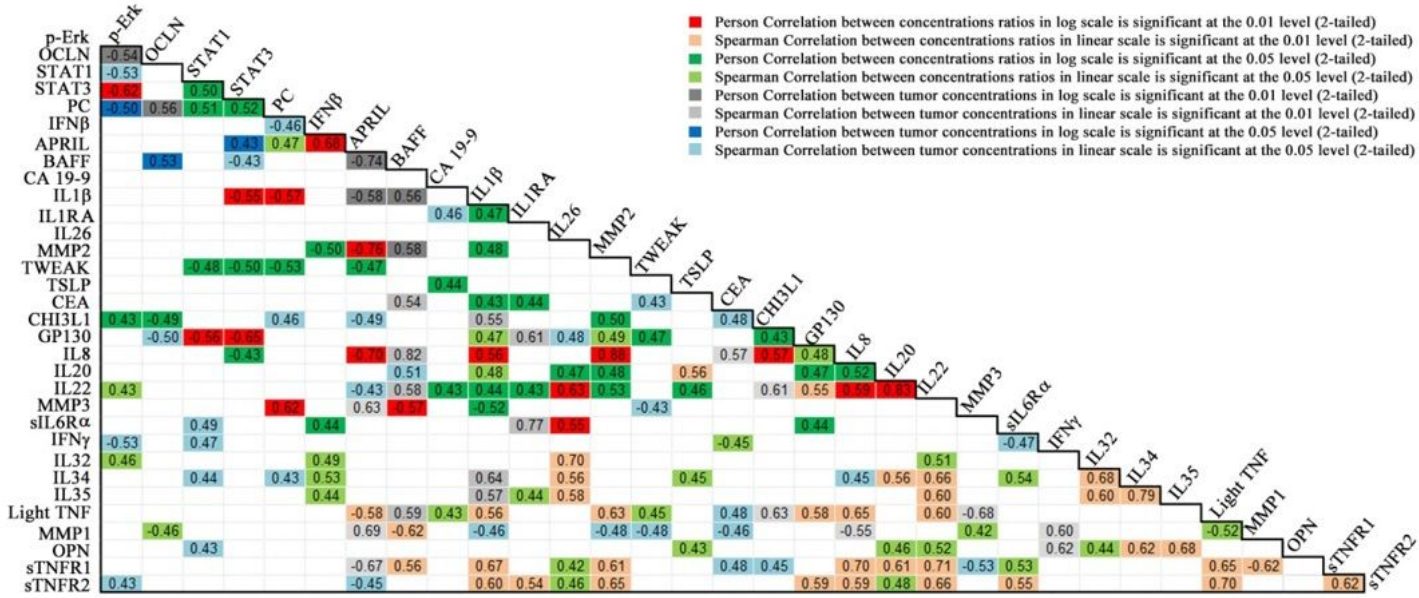

Figure 3

Combined multi-type variables correlation matrix containing the highest values of the correlation coefficients. The combinations between the two levels of significance (0.01 and 0.05) and the calculation methods (Pearson or Spearman) is color-coded, as showed by the legend in the upper-right of the matrix. See Supplementary Figure S5 for protein carbonyl immunoblot examples.

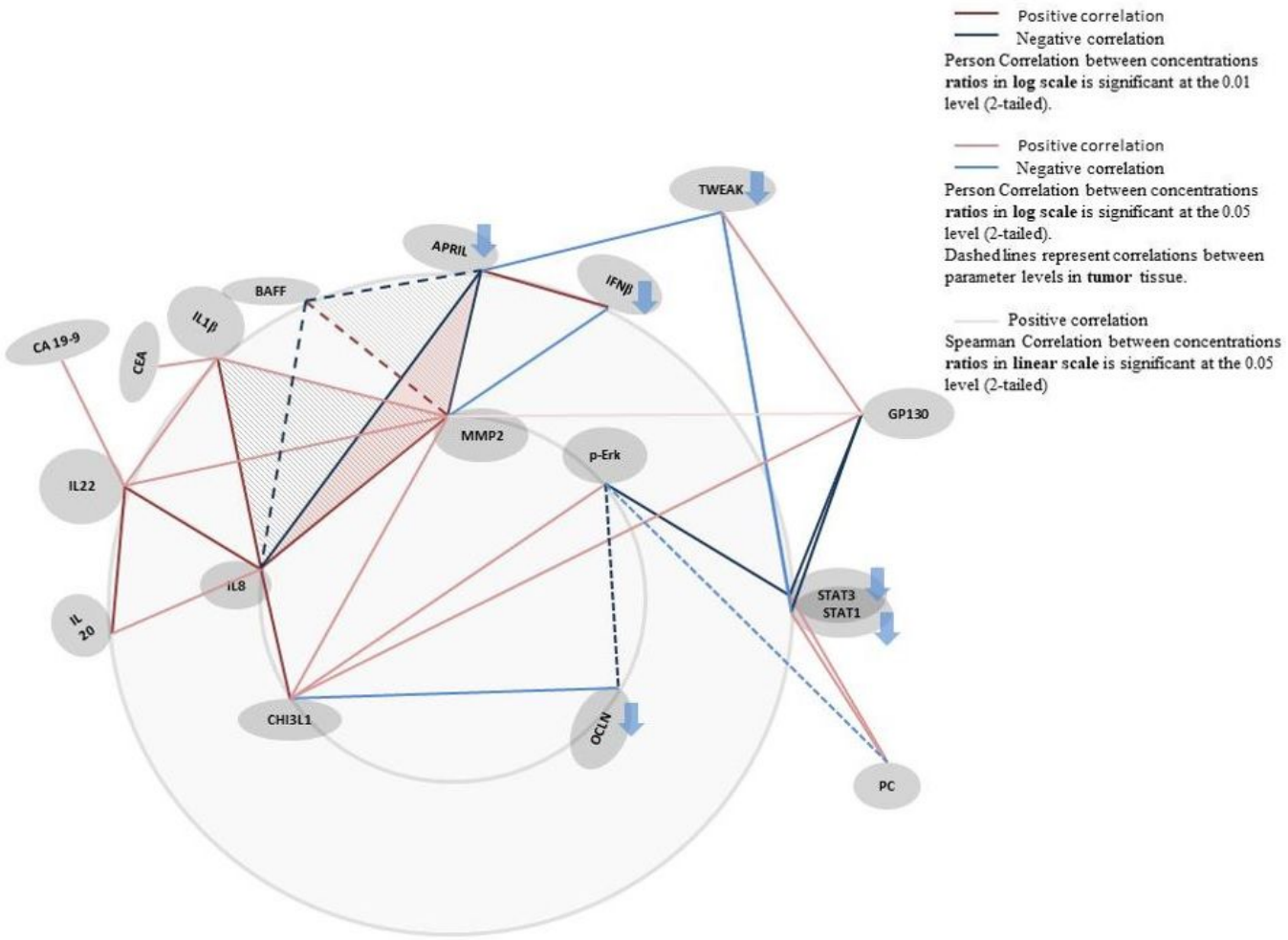

Figure 4

Statistically significant correlated clusters of biomarkers connected according to their two by two correlation significance levels.

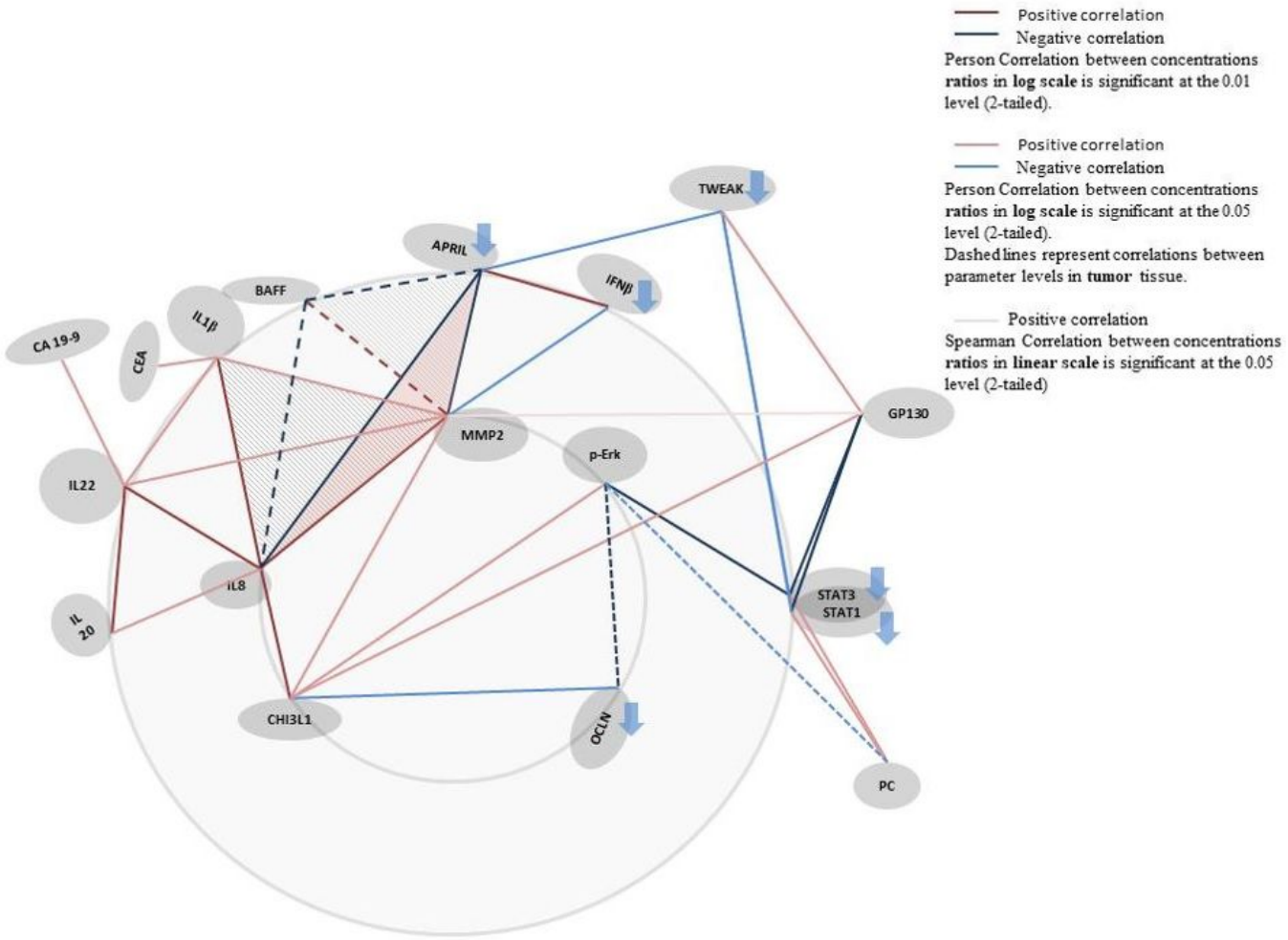

Figure 4

Statistically significant correlated clusters of biomarkers connected according to their two by two correlation significance levels.

Supplementary Files

This is a list of supplementary files associated with this preprint. Click to download.

- Supplementaryinformation.pdf
- Supplementaryinformation.pdf